Eur J Pediatr
DOI 10.1007/s00431-009-1126-6

ORIGINAL PAPER

Successful cord blood transplantation for a CHARGE syndrome with *CHD7* mutation showing DiGeorge sequence including hypoparathyroidism

Hirosuke Inoue · Hidetoshi Takada · Takeshi Kusuda · Takako Goto · Masayuki Ochiai · Tadamune Kinjo · Jun Muneuchi · Yasushi Takahata · Naomi Takahashi · Tomohiro Morio · Kenjiro Kosaki · Toshiro Hara

Received: 22 July 2009 / Accepted: 1 December 2009

Abstract It is rare that coloboma, heart anomalies, choanal atresia, retarded growth and development, and genital and ear anomalies (CHARGE) syndrome patients have DiGeorge sequence showing severe immunodeficiency due to the defect of the thymus. Although the only treatment to achieve immunological recovery for these patients in countries where thymic transplantation is not ethically approved would be hematopoietic cell transplantation, long-term survival has not been obtained in most patients. On the other hand, it is still not clarified whether hypoparathyroidism is one of the manifestations of CHARGE syndrome. We observed a CHARGE syndrome patient with chromodomain helicase DNA-binding protein 7 mutation showing DiGeorge sequence including the defect of T cells accompanied with the aplasia of the thymus, severe hypoparathyroidism, and conotruncal cardiac anomaly. He received unrelated cord blood transplantation without conditioning at 4 months of age. Recovery of T cell number and of proliferative response against mitogens was achieved by peripheral expansion of mature T cells in cord blood without thymic output. Although he is still suffering from severe hypoparathyroidism, he is alive without serious infections for 10 months.

Keywords CHARGE syndrome · DiGeorge sequence · *CHD7* mutation · Hypoparathyroidism · Cord blood transplantation

Abbreviations

CHD7	Chromodomain helicase DNA-binding protein 7
CBT	Cord blood transplantation
TCR	T cell receptor
PHA	Phytohemagglutinin
Con A	Concanavalin A
ABR	Auditory brainstem response
GVHD	Graft versus host disease

Introduction

Coloboma, heart anomalies, choanal atresia, retarded growth and development, and genital and ear anomalies (CHARGE) syndrome is a distinctive clinical entity with multiple congenital anomalies [12]. Mutations in the gene chromodomain helicase DNA-binding protein 7 (*CHD7*) were identified as a cause of CHARGE syndrome [25]. *CHD7* on chromosome 8 (8q12.1) is a member of the chromodomain helicase DNA binding domain family [25]. Chromatin remodeling is a recognized mechanism of gene expression regulation, and the *CHD7* gene is likely to play a significant role in embryonic development and cell cycle regulation [29]. CHD7 is expressed throughout the neural crest containing mesenchyme of the pharyngeal arches. Mouse embryo at 10.5 days postcoitum expressed *Chd7* in

H. Inoue · H. Takada (✉) · T. Kusuda · T. Goto · M. Ochiai · T. Kinjo · J. Muneuchi · Y. Takahata · T. Hara
Department of Pediatrics, Graduate School of Medical Sciences, Kyushu University,
3-1-1 Maidashi, Higashi-ku,
Fukuoka 812-8582, Japan
e-mail: takadah@pediatr.med.kyushu-u.ac.jp

N. Takahashi · T. Morio
Department of Pediatrics and Developmental Biology, Graduate School of Medical and Dental Sciences, Tokyo Medical and Dental University, Tokyo, Japan

K. Kosaki
Department of Pediatrics, School of Medicine, Keio University, Tokyo, Japan

Published online: 06 January 2010

the cardiac outflow tract, truncus arteriosus, facio-acoustic preganglion complex, hindbrain, forebrain, mandibular component of the first branchial arch, otic vesicle, optic stalk/optic vesicle, and olfactory pit [12]. Thus, CHARGE syndrome has the potential of multiple presentations.

Cellular immunodeficiency due to the lack of the thymus is not widely recognized as a manifestation of CHARGE syndrome. Recently, severe hypoparathyroidism and conotruncal cardiac anomaly were reported in patients with CHARGE syndrome caused by *CHD7* mutations having DiGeorge sequence characterized by the defect of T cells accompanied by thymus aplasia [21, 28, 30]. Although thymus hypoplasia or agenesis is rare in postnatal CHARGE syndrome cases [3], Sanlaville et al. reported that it was observed in seven of ten CHARGE syndrome fetuses [22]. Recently, Jyonouchi et al. reported that 8% (two of 25) of CHARGE syndrome patients had a phenotype of severe combined immunodeficiency with defect of T cells [10]. On the other hand, it is still not clarified whether hypoparathyroidism is one of the manifestations of CHARGE syndrome since only three CHARGE syndrome patients with *CHD7* mutation were reported to have hypoparathyroidism [21, 28, 30]. It is suggested that neural crest defect underlies the clinical overlap of both chromosome 22q11 deletion and CHARGE syndrome [22]. Accordingly, a case manifesting the CHARGE syndrome with deletion in chromosome 22q11 was reported [7].

Here, we report a patient with CHARGE syndrome with a *CHD7* mutation, who had severe T cell immune deficiencies due to thymic aplasia, severe limb anomalies, and congenital hypoparathyroidism. He was successfully treated with cord blood transplantation (CBT).

Case report

The patient was born at 39 weeks of gestational age. His birth weight was 2,488 g. Cardiac anomaly and polyhydramnion were detected by fetal ultrasound examination during his late prenatal period. Karyotype analysis of amniotic fluid showed 46,XY. His family members were healthy without having even minor anomalies.

Shortly after birth, he was admitted to the neonatal intensive care unit (NICU) in Kyushu University Hospital. He showed the characteristic facial features such as a hypertelorism and unilateral facial palsy (Fig. 1a), asymmetry of ears with protruding, helix hypoplasia, low-set and square-shaped right ear, absent anthelix, low-set left ear (Fig. 1b, c), and bilateral coloboma of the choroid. In addition, thumb polydactyly and cleft of the right hand and cleft and cutaneous syndactyly of the bilateral feet were observed (Fig. 1d–g). He had no genital abnormalities. Hematological examinations revealed white blood cell count of 4,330/μl with severe lymphopenia (neutrophils 68.5%, lymphocytes 7%, monocytes 18%). Serum calcium, phosphorus, and parathyroid hormone levels were 7.8 mg/dl, 8.4 mg/dl, and 4.5 pg/ml, respectively, showing hypoparathyroidism. Serum thyroid hormone levels were normal. Lymphocyte surface marker analysis by a flow cytometer revealed a marked decrease of T lymphocytes: $CD3^+$ 2.8% (8 cells/μl), $CD4^+$ 2.3% (7 cells/μl), and $CD8^+$ 15.3% (46 cells/μl; Table 1). T cell receptor (TCR) $\gamma\delta^+$ cells, $CD16^+/CD56^+$ cells, and $CD19^+$ cells were 0.1%, 35.9%, and 52.9%, respectively. Proliferative response of mononuclear cells against phytohemagglutinin (PHA) and concanavalin A (Con A) was 123 %S.I. (normal controls; 254–388) and 2,530 cpm (20,300–65,700), respectively. Analysis of the TCRVβ repertoire showed an abnormal pattern with overexpansion of $V\beta21.3^+$ cells (20.9%; Fig. 2a). Serum IgG, IgA, and IgM concentrations were 899, 5, and 19 mg/dl, respectively. Fluorescent in situ hybridization analysis revealed a lack of maternal cell engraftment in peripheral blood and no deletion at 22q11.2.

Computed tomography and fiberoptic laryngoscope examination revealed left choanal atresia with posterior choanal stenosis and laryngomalacia, respectively. Auditory brainstem response revealed bilateral severe sensorineuronal hearing loss. An echocardiogram and chest computed tomography scan revealed truncus arteriosus (Van Praagh type A4) and interruption of aortic arch (type B) with aberrant right subclavian artery. At 14 days of age, he underwent bilateral pulmonary artery banding operation because he was too small to receive the radical correction of truncus arteriosus and interruption of aortic arch at that time. Thymus was not detected at the time of operation.

Thus, we made the clinical diagnosis of CHARGE syndrome with manifestations of complete-type athymic DiGeorge sequence. The *CHD7* gene of the patient was analyzed according to the method described previously [2], and heterozygous c.1036A > T (R346X) mutation was observed in exon 2. He received unrelated CBT without conditioning at 4 months of age (Fig. 2b). Human leukocyte antigen full-matched female cord blood cells (28.03×10^7 cells/kg) were infused. FK506 and short-term methotrexate were used for graft versus host disease (GVHD) prophylaxis. He had only mild skin manifestation of GVHD, which resolved by prednisolone (1 mg/kg/day). On day 25 after CBT, $CD3^+$ cells increased to 60.1% of lymphocytes (1,471 cells/μl), 93.8% of which were positive for CD45RO. Analysis of the TCRVβ repertoire on day 27 showed an abnormal pattern with overexpansion of $V\beta16^+$ cells (7.3%) and $V\beta17^+$ cells (9.7%), and a different profile was observed between pre-CBT and post-CBT (Fig. 2a). Proliferative response to Con A and PHA normalized on day 50 (20,500 cpm) and on day 174 (284 %S.I.), respectively. Chimerism analysis on day 173 showed that most of the $CD3^+$

Fig. 1 Clinical manifestations of the patients. **a** Frontal view of the face showing hypertelorism and right facial palsy. **b** Lateral view of the right ear showing protruding, helix hypoplasia, and low-set ear. **c** Lateral view of the left ear showing square-shaped, absent anthelix, and low-set ear. Note asymmetry of ears. **d** Thumb polydactyly and cleft of the right hand. **e** Normal left hand. **f, g** Cleft and cutaneous syndactyly of the bilateral foots. Written consent was obtained for publication of these pictures

cells were of donor origin (94.5% of $CD3^+$ cells were XX, 5.5% were XY). At 10 months of age (day 169 after CBT), $CD3^+$ cells were 36.3% of lymphocytes (973 cells/μl), and 86.2% of T cells were positive for CD45RO. T cell receptor excision circles were below the detection limit before CBT, confirming the lack of thymic output (data not shown).

He is alive without serious infections with regular administration of immunoglobulin and prophylactic antibiotics. At 10 months of age, serum calcium, phosphorus, and parathyroid hormone levels are 7.2 mg/dl, 6.1 mg/dl, and 3.0 pg/ml, respectively. He is still receiving calcium preparation and alfacalcidol.

Table 1 Immunological studies

	Pretransplantation	Posttransplantation
$CD3^+$ cells (% lymphocytes)	2.8	36.3
$CD3^+$ cells (cells/μl)	8	973
$CD45RO^+/CD3^+$ (%)	87.7	86.2
$CD45RO^-/CD3^+$ (%)	12.4	10.9
$CD4^+$ cells (% lymphocytes)	2.3	24.2
$CD4^+$ cells (cells/μl)	7	648
$CD8^+$ cells (% lymphocytes)	15.3	12.1
$CD8^+$ cells (cells/μl)	46	324
TCR $\gamma\delta^+$ (%)	0.1	0.2
$CD19^+$ (%)	52.9	33.3
$CD16^+/CD56^+$ (%)	35.9	29.7
Proliferative response		
Against PHA (%S.I.)	123	284
Against Con A (cpm)	2,530	20,500
IgG (mg/dl)	899	425
IgM (mg/dl)	19	83
IgA (mg/dl)	5	66
Karyotype of $CD3^+$ cells	99.5% of 46,XY	5.5% of 46,XY
	0.5% of 46,XX	94.5% of 46,XX

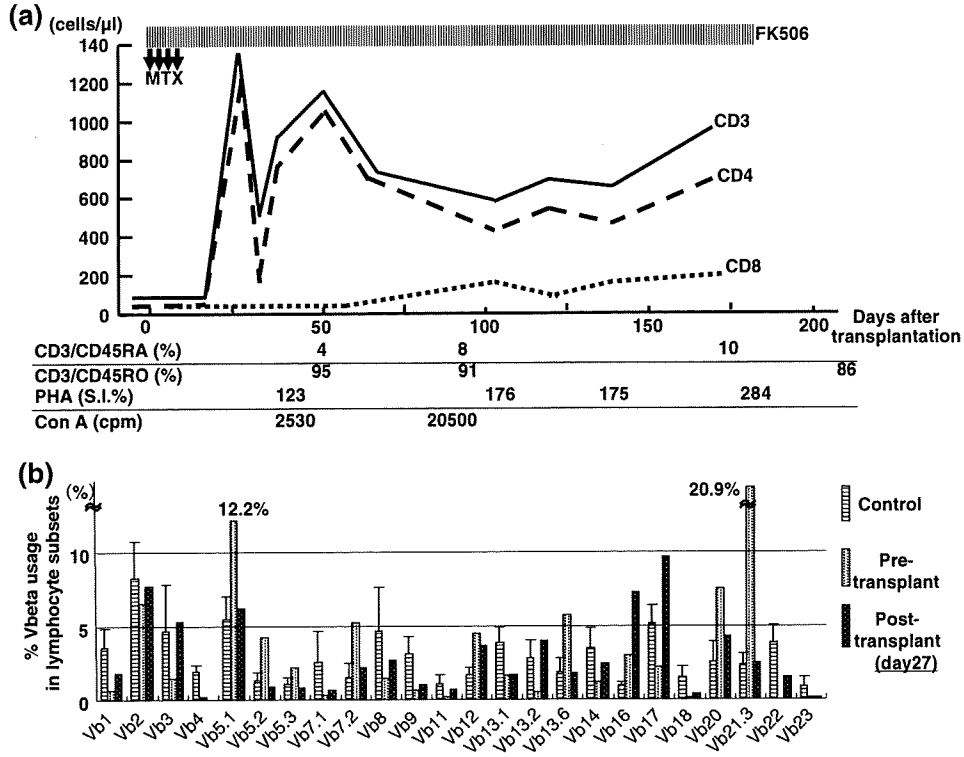

Fig. 2 Clinical course and immunological recovery after the cord blood transplantation. **a** Clinical course of the cord blood transplantation. *MTX* methotrexate, *PHA* phytohemagglutinin, *Con A* concanavalin A. **b** TCRVβ repertoire profile on the patient and control subjects. Note the skewing in the TCR repertoire before and after transplantation. *TCR* T cell receptor

Discussion

Our patient showed absence of T lymphocytes accompanied with aplasia of the thymus manifesting complete-type DiGeorge sequence, a rare complication of CHARGE syndrome [1, 30]. T cell number of the patient was recovered by CBT, although most of the T cells showed memory phenotype reflecting peripheral expansion of donor cord blood-derived mature T cells and the lack of the thymic output. He presented with additional rare manifestations, severe limb anomalies, and congenital hypoparathyroidism. DiGeorge sequence is associated with a deletion of chromosome 22q11.2 in approximately 80% of patients [23]. Interestingly, Markert et al. reported that only 52% of 54 patients with DiGeorge sequence had a deletion of 22q11, and 26% had CHARGE phenotype without the deletion [15]. A number of genes have been identified in the 22q11.2 region [31], including *TBX1* that is a major genetic determinant of del22q11.2 syndrome. As TBX1 is a transcription factor that contains a DNA binding domain, it is possible that TBX1 is a functional target for CHD7.

Thymic hypo/agenesis was observed in 70% of fetuses with CHARGE syndrome [22]. The high frequency of thymic defect in fetuses suggests that accompanying immune deficiency may be more common in this disease than previously reported. It is possible that many of athymic patients were counted on DiGeorge syndrome, rather than CHARGE syndrome. Otherwise, CHARGE syndrome patients with thymic defect may more often die during perinatal period because of the immunodeficiency or other accompanying anomalies such as severe cardiac defect. Although there have been a few reports of stem cell transplantation for the treatment of T cell deficiency in complete-type DiGeorge sequence, this is the first case of CBT for the treatment of CHARGE syndrome with *CHD7* mutation manifesting T cell defect [8, 14, 18]. The optimal treatment for patients with complete-type DiGeorge sequence has not been established. In the absence of treatment, patients usually die in the first 2 years of life [16]. Therefore, prompt reconstitution of the immune function is required to prevent fatal infectious complications. The common treatments for immunological reconstitution in complete-type DiGeorge sequence are thymic and bone marrow transplantation [13, 15]. Although thymic transplantation would be more reasonable from the physiological point of view, it is not ethically approved in Japan. We selected CBT without conditioning regimen for our patient because of the following reasons: (1) lack of sibling donors, (2) more noninvasive procurement and more rapid availability than the matched unrelated donors, (3) lower risk of GVHD or viral transmission in CBT compared with bone marrow or peripheral blood stem cells [5], and (4) higher frequency of naïve T cells in cord blood [6], which have a longer lifespan than their memory counterparts [26]. Because of the lack of thymic output after the transplantation in this disease, the high frequency of naïve T cells in the donor cells may be an important factor to avoid early immune senescence. On the other hand, it may take more time for the recovery of neutrophils in CBT leaving a higher risk of infection compared with bone marrow or peripheral stem cell transplantation [5]. In addition, naïve T cells in cord blood may require a longer time to mature into effecter memory cells and thus do not provide immediate defense against microbial agents [11]. Our patient received CBT in the NICU and has been bred in a closed infant incubator since birth. This might in part contribute to the decrease of the risk of infections and to the success of CBT.

Ryan et al. [20] reported that only a few patients (1–4%) had mild limb abnormalities in 548 patients with chromosome 22q11 deletions. Limb anomalies were not initially described in CHARGE syndrome [4]. Recently, limb anomalies have been reported as a rare manifestation in CHARGE syndrome [3, 17, 19]. On the other hand, Brock et al. [4] reported that limb anomalies occurred in about 30% of patients with definite or probable CHARGE syndrome. It is interesting that limb anomalies with DiGeorge sequence are more frequently observed in male (P value <0.034), and limb anomalies were observed in 70.0% of male DiGeorge sequence with definite CHARGE syndrome [4]. Williams proposed that CHARGE syndrome is caused by a disruption of mesenchymal–epithelial (including ectoderm and endoderm) interaction [27]. Sanlaville et al. [22] showed that the *CHD7* gene is also expressed in the limb bud mesenchyme during embryogenesis. Van de Laar et al. [24] reported that three CHARGE syndrome patients with CHD7 mutation had severe limb anomalies. Therefore, it is possible that *CHD7* mutation itself is responsible for limb defects, and limb anomalies are more strongly associated with *CHD7* mutation than 22q11 deletion.

In patients with 22q11 deletion, 203 of 340 (60%) had hypoparathyroidism and hypocalcaemia, and the hypocalcaemia resolved in 70% [20]. On the other hand, only three CHARGE syndrome patients with *CHD7* mutations had hypoparathyroidism [21, 28, 30]. It is interesting that the three patients had severe T cell deficiency [21, 28, 30]. As TBX1 might be a functional target of CHD7, it is possible that hypoparathyroidism may be more common in CHARGE syndrome than previously recognized. Günther et al. showed by using *glial cells missing2*-deficient mice that thymus had a backup mechanism of parathyroid gland and thymus itself secreted parathyroid hormone when parathyroid glands was absent [9]. It is possible that intractable hypocalcemia continues when both parathyroid gland and thymus are absent.

CHARGE syndrome is a complex of congenital malformations, and the acronym CHARGE presents the cardinal features of the disorder. Recently, there are several reports about complications with CHARGE syndrome such as immunodeficiency, limb anomaly, and parathyroid gland deficiency, which were not well recognized previously. In particular, immunodeficiency caused by thymus defect as well as the heart anomalies may be a fatal complication in this syndrome. This disease should be diagnosed as early as possible, and the immunological evaluation should be performed carefully. When the patients have severe T cells deficiency, prompt immunological reconstitution should be undertaken appropriately. Careful observation would be necessary for the gradual exhaustion of T cells and the development of autoimmune and malignant diseases in these patients after stem cell transplantation.

Conflict of interest The authors declare that there was no financial support that might pose a conflict of interest in connection with the submitted article.

References

1. Aramaki M, Udaka T, Kosaki R et al (2006) Phenotypic spectrum of CHARGE syndrome with CHD7 mutations. J Pediatr 148 (3):410–414
2. Aramaki M, Udaka T, Torii C et al (2006) Screening for CHARGE syndrome mutations in the CHD7 gene using denaturing high-performance liquid chromatography. Genet Test 10(4):244–251
3. Blake KD, Davenport SL, Hall BD et al (1998) CHARGE association: an update and review for the primary pediatrician. Clin Pediatr (Phila) 37(3):159–173
4. Brock KE, Mathiason MA, Rooney BL et al (2003) Quantitative analysis of limb anomalies in CHARGE syndrome: correlation with diagnosis and characteristic CHARGE anomalies. Am J Med Genet A 123A(1):111–121
5. Brown JA, Boussiotis VA (2008) Umbilical cord blood transplantation: basic biology and clinical challenges to immune reconstitution. Clin Immunol 127(3):286–297
6. D'Arena G, Musto P, Cascavilla N et al (1998) Flow cytometric characterization of human umbilical cord blood lymphocytes: immunophenotypic features. Haematologica 83(3):197–203
7. Devriendt K, Swillen A, Fryns JP (1998) Deletion in chromosome region 22q11 in a child with CHARGE association. Clin Genet 53 (5):408–410
8. Gennery AR, Slatter MA, Rice J et al (2008) Mutations in *CHD7* in patients with CHARGE syndrome cause T-B + natural killer cell + severe combined immune deficiency and may cause Omenn-like syndrome. Clin Exp Immunol 153(1):75–80
9. Günther T, Chen ZF, Kim J et al (2000) Genetic ablation of parathyroid glands reveals another source of parathyroid hormone. Nature 406(6792):199–203
10. Jyonouchi S, McDonald-McGinn DM, Bale S et al (2009) CHARGE (coloboma, heart defect, atresia choanae, retarded growth and development, genital hypoplasia, ear anomalies/ deafness) syndrome and chromosome 22q11.2 deletion syndrome: a comparison of immunologic and nonimmunologic phenotypic features. Pediatrics 123(5):e871–e877
11. Komanduri KV, St John LS, de Lima M et al (2007) Delayed immune reconstitution after cord blood transplantation is characterized by impaired thymopoiesis and late memory T-cell skewing. Blood 110 (13):4543–4551
12. Lalani SR, Safiullah AM, Fernbach SD et al (2006) Spectrum of *CHD7* mutations in 110 individuals with CHARGE syndrome and genotype–phenotype correlation. Am J Hum Genet 78(2):303–314
13. Land MH, Garcia-Lloret MI, Borzy MS et al (2007) Long-term results of bone marrow transplantation in complete DiGeorge syndrome. J Allergy Clin Immunol 120(4):908–915
14. Markert ML (2008) Treatment of infants with complete DiGeorge anomaly. J Allergy Clin Immunol 121(4):1063–1064
15. Markert ML, Devlin BH, Alexieff MJ et al (2007) Review of 54 patients with complete DiGeorge anomaly enrolled in protocols for thymus transplantation: outcome of 44 consecutive transplants. Blood 109(10):4539–4547
16. Markert ML, Hummell DS, Rosenblatt HM et al (1998) Complete DiGeorge syndrome: persistence of profound immunodeficiency. J Pediatr 132(1):15–21
17. Meinecke P, Polke A, Schmiegelow P (1989) Limb anomalies in the CHARGE association. J Med Genet 26(3):202–203
18. Ohtsuka Y, Shimizu T, Nishizawa K et al (2004) Successful engraftment and decrease of cytomegalovirus load after cord blood stem cell transplantation in a patient with DiGeorge syndrome. Eur J Pediatr 163(12):747–748
19. Prasad C, Quackenbush EJ, Whiteman D et al (1997) Limb anomalies in DiGeorge and CHARGE syndromes. Am J Med Genet 68(2):179–181
20. Ryan AK, Goodship JA, Wilson DI et al (1997) Spectrum of clinical features associated with interstitial chromosome 22q11 deletions: a European collaborative study. J Med Genet 34(10):798–804
21. Sanka M, Tangsinmankong N, Loscalzo M et al (2007) Complete DiGeorge syndrome associated with CHD7 mutation. J Allergy Clin Immunol 120(4):952–954
22. Sanlaville D, Etchevers HC, Gonzales M et al (2006) Phenotypic spectrum of CHARGE syndrome in fetuses with CHD7 truncating mutations correlates with expression during human development. J Med Genet 43(3):211–217
23. Sullivan KE (2004) The clinical, immunological, and molecular spectrum of chromosome 22q11.2 deletion syndrome and DiGeorge syndrome. Curr Opin Allergy Clin Immunol 4(6):505–512
24. Van de Laar I, Dooijes D, Hoefsloot L et al (2007) Limb anomalies in patients with CHARGE syndrome: an expansion of the phenotype. Am J Med Genet A 143A(22):2712–2715
25. Vissers LE, van Ravenswaaij CM, Admiraal R et al (2004) Mutations in a new member of the chromodomain gene family cause CHARGE syndrome. Nat Genet 36(9):955–957
26. Vrisekoop N, den Braber I, de Boer AB et al (2008) Sparse production but preferential incorporation of recently produced naive T cells in the human peripheral pool. Proc Natl Acad Sci USA 105(16):6115–6120
27. Williams MS (2005) Speculations on the pathogenesis of CHARGE syndrome. Am J Med Genet A 133A(3):318–325
28. Wincent J, Holmberg E, Strömland K et al (2008) CHD7 mutation spectrum in 28 Swedish patients diagnosed with CHARGE syndrome. Clin Genet 74(1):31–38
29. Woodage T, Basrai MA, Baxevanis AD et al (1997) Characterization of the CHD family of proteins. Proc Natl Acad Sci USA 94 (21):11472–11477
30. Writzl K, Cale CM, Pierce CM et al (2007) Immunological abnormalities in CHARGE syndrome. Eur J Med Genet 50 (5):338–345
31. Yagi H, Furutani Y, Hamada H et al (2003) Role of TBX1 in human del22q11.2 syndrome. Lancet 362(9393):1366–1373

Immunology
The Journal of cells, molecules, systems and technologies
British Society for immunology

IMMUNOLOGY ORIGINAL ARTICLE

Ex vivo expanded cord blood CD4 T lymphocytes exhibit a distinct expression profile of cytokine-related genes from those of peripheral blood origin

Yoshitaka Miyagawa,[1] Nobutaka Kiyokawa,[1] Nakaba Ochiai,[2,3] Ken-Ichi Imadome,[4] Yasuomi Horiuchi,[1] Keiko Onda,[1] Misako Yajima,[4] Hiroyuki Nakamura,[4] Yohko U. Katagiri,[1] Hajime Okita,[1] Tomohiro Morio,[2,5] Norio Shimizu,[2,6] Junichiro Fujimoto[7] and Shigeyoshi Fujiwara,[4]

[1]*Department of Developmental Biology, National Research Institute for Child Health and Development, Setagaya-ku,* [2]*Center for Cell Therapy, Tokyo Medical and Dental University Medical Hospital, Bunkyo-ku, Tokyo,* [3]*Lymphotec Inc., Koto-ku, Tokyo,* [4]*Department of Infectious Diseases, National Research Institute for Child Health and Development, Setagaya-ku, Tokyo,* [5]*Department of Pediatrics and Developmental Biology, Graduate School of Medicine, Tokyo Medical and Dental University, Bunkyo-ku, Tokyo,* [6]*Department of Virology, Division of Medical Science, Medical Research Institute, Tokyo Medical and Dental University, Bunkyo-ku, Tokyo, and* [7]*Vice Director General, National Research Institute for Child Health and Development, Setagaya-ku, Tokyo, Japan*

doi:10.1111/j.1365-2567.2009.03122.x
Received 1 September 2008; revised 30 March 2009; accepted 15 April 2009.
Correspondence: N. Kiyokawa, MD, PhD, Department of Developmental Biology, National Research Institute for Child Health and Development, 2-10-1, Okura, Setagaya-ku, Tokyo 157-8535, Japan.
Email: nkiyokawa@nch.go.jp
Senior author: Nobutaka Kiyokawa

Summary

With an increase in the importance of umbilical cord blood (CB) as an alternative source of haematopoietic progenitors for allogenic transplantation, donor lymphocyte infusion (DLI) with donor CB-derived activated $CD4^+$ T cells in the unrelated CB transplantation setting is expected to be of increased usefulness as a direct approach for improving post-transplant immune function. To clarify the characteristics of activated $CD4^+$ T cells derived from CB, we investigated their mRNA expression profiles and compared them with those of peripheral blood (PB)-derived activated $CD4^+$ T cells. Based on the results of a DNA microarray analysis and quantitative real-time reverse transcriptase–polymerase chain reaction (RT-PCR), a relatively high level of forkhead box protein 3 (Foxp3) gene expression and a relatively low level of interleukin (IL)-17 gene expression were revealed to be significant features of the gene expression profile of CB-derived activated $CD4^+$ T cells. Flow cytometric analysis further revealed protein expression of Foxp3 in a portion of CB-derived activated $CD4^+$ T cells. The low level of retinoic acid receptor-related orphan receptor γ isoform t (RORγt) gene expression in CB-derived activated $CD4^+$ T cells was speculated to be responsible for the low level of IL-17 gene expression. Our data indicate a difference in gene expression between $CD4^+$ T cells from CB and those from PB. The findings of Foxp3 expression, a characteristic of regulatory T cells, and a low level of IL-17 gene expression suggest that CB-derived $CD4^+$ T cells may be a more appropriate source for DLI.

Keywords: CD4; cord blood; donor lymphocyte infusion; forkhead box protein 3; interleukin 17; T cell

Abbreviations: BIM, BCL2-like 11; CB, cord blood; CTLA-4, cytotoxic T-lymphocyte antigen-4; CDKN, cyclin-dependent kinase inhibitor; DLI, donor lymphocyte infusion; Foxp3, forkhead box protein 3; GAPDH, glyceraldehyde-3-phosphate dehydrogenase; GM-CSF, granulocyte–macrophage colony-stimulating factor; GVHD, graft-versus-host disease; GVL, graft-versus-leukaemia; HSCT, haematopoietic stem cell transplantation; ICOS, inducible T-cell co-stimulator; IFNG, interferon γ; IL, interleukin; PB, peripheral blood; RORγt, retinoic acid receptor-related orphan receptor γ isoform t; RT, reverse transcriptase; TCR, T-cell receptor; Th, T helper cell; Treg, regulatory T cell.

Introduction

Donor lymphocyte infusion (DLI) is a direct and useful approach for improving post-transplant immune function. DLI has been shown to exert a graft-versus-leukaemia (GVL) effect and has emerged as an effective strategy for the treatment of patients with leukaemia, especially chronic myelogenous leukaemia, who have relapsed after unrelated haematopoietic stem cell transplantation (HSCT).[1] In addition, DLI has been successfully used for some life-threatening viral infections, including Epstein–Barr virus and cytomegalovirus infections after HSCT.[2]

Although DLI frequently results in significant acute and/or chronic graft-versus-host disease (GVHD), several groups have demonstrated that depletion of CD8 T cells from DLIs efficiently reduces the incidence and severity of GVHD while maintaining GVL activity.[3,4] Therefore, selective CD4 DLI is expected to provide an effective and low-toxicity therapeutic strategy for improving post-transplant immune function. Actually, selective CD4 DLI based on a recently established method for *ex vivo* T-cell expansion using anti-CD3 monoclonal antibody and interleukin (IL)-2 is now becoming established as a routine therapeutic means of resolving post-transplant immunological problems in Japan.[5]

The importance of umbilical cord blood (CB) as an alternative source of haematopoietic progenitors for allogenic transplantation, mainly in patients lacking a human leucocyte antigen (HLA)-matched marrow donor, has increased in recent years. Because of the naïve nature of CB lymphocytes, the incidence and severity of GVHD are reduced in comparison with the allogenic transplant setting. In addition, CB is rich in primitive $CD16^-$ $CD56^+$ natural killer (NK) cells, which possess significant proliferative and cytotoxic capacities, and so have a substantial GVL effect.[6]

In contrast, a major disadvantage of CB transplantation is the low yield of stem cells, resulting in higher rates of engraftment failure and slower engraftment compared with bone marrow transplantation. In addition, it was generally thought to be difficult to perform DLI after CB transplantation using donor peripheral blood (PB), with the exception of transplantations from siblings. However, the above-described method for the *ex vivo* expansion of activated T cells can produce a sufficient amount of cells for therapy using the CB cell residues in an infused bag, which has solved this problem and made it possible to perform DLI with donor CB-derived activated $CD4^+$ T cells in the unrelated CB transplantation setting.[5] It has also been reported that CB-derived T cells can be expanded *ex vivo* while retaining the naïve and/or central memory phenotype and polyclonal T-cell receptor (TCR) diversity,[7] and thus potential utilization for adoptive cellular immunotherapy post-CB transplantation has been suggested.[8]

There are functional differences between CB and PB lymphocytes, although the details remain unclear. In an attempt to clarify the differences in characteristics between activated $CD4^+$ T cells derived from CB and those derived from PB, we investigated gene expression profiles. In this paper we present evidence that CB-derived $CD4^+$ T cells are distinct from PB-derived $CD4^+$ T cells in terms of gene expression.

Materials and methods

Cell culture and preparation

CB was distributed by the Tokyo Cord Blood Bank (Tokyo, Japan). The CB was originally collected and stored for stem cell transplantation. Stocks that were inappropriate for transplantation because they contained too few cells were distributed for research use with informed consent, with the permission of the ethics committee of the bank. In addition, all of the experiments in this study using distributed CB were performed with the approval of the local ethics committee. The mononuclear cells were isolated by Ficoll-Paque centrifugation and cultured in the presence of an anti-CD3 monoclonal antibody and interleukin (IL)-2 using TLY Culture Kit 25 (Lymphotec Inc., Tokyo, Japan) as described previously.[5] Although several different methods for T-cell stimulation have been reported, this method is currently being used clinically in Japan. Thus we selected this method in this study. After 14 days of culture, $CD4^+$ cells were isolated using a magnetic-activated cell sorting (MACS) system (Miltenyi Biotec, Bergisch Gladbach, Germany) according to the manufacturer's instructions. As a control, mononuclear cells isolated from the peripheral blood of healthy volunteers were similar examined.

Polymerase chain reaction (PCR)

Total RNA was extracted from cells using an RNeasy kit (Qiagen, Valencia, CA) and reverse-transcribed using a First-Strand cDNA synthesis kit (GE Healthcare Bio-Science Corp., Little Chalfont, Buckinghamshire, UK) according to the manufacturer's instructions. Using cDNA synthesized from 150 ng of total RNA as a template for one amplification, real-time reverse transcriptase (RT)-PCR was performed using SYBR® Green PCR master mix, TaqMan® Universal PCR master mix and TaqMan® gene expression assays (Applied Biosystems, Foster City, CA), and an inventoried assay carried out on an ABI PRISM® 7900HT sequence detection system (Applied Biosystems) according to the instructions provided. Either the glyceraldehyde-3-phosphate dehydrogenase (GAPDH) gene or the β-actin gene was used as an internal control for normalization. The sequences of gene-specific primers for real-time RT-PCR are listed in Table 1.

DNA microarray analysis

The microarray analysis was performed as previously described.[9] Total RNA isolated from cells was reverse-

Table 1. The sequences of gene-specific primers for reverse transcriptase–polymerase chain reaction (RT-PCR) and real-time RT-PCR used in this study

Primer	Sequence
IL-4 forward	CACAGGCACAAGCAGCTGAT
IL-4 reverse	CCTTCACAGGACAGGAATTCAAG
IL-6 forward	GTAGCCGCCCCACACAGA
IL-6 reverse	CCGTCGAGGATGTACCGAAT
IL-10 forward	GCCAAGCCTTGTCTGAGATGA
IL-10 reverse	CTTGATGTCTGGGTCTTGGTTCT
IL-17 forward	GACTCCTGGGAAGACCTCATTG
IL-17 reverse	TGTGATTCCTGCCTTCACTATGG
IL-17F forward	GCTTGACATTGGCATCATCAA
IL-17F reverse	GGAGCGGCTCTCGATGTTAC
IL-23 forward	GAGCCTTCTCTGCTCCCTGATAG
IL-23 reverse	AGTTGGCTGAGGCCCAGTAG
IL-23R forward	AACAACAGCTCGGCTTTGGTATA
IL-23R reverse	GGGACATTCAGCAGTGCAGTAC
IFNG forward	CATCCAAGTGATGGCTGAACTG
IFNG reverse	TCGAAACAGCATCTGACTCCTTT
GM-CSF forward	CAGCCCTGGAGCATGTG
GM-CSF reverse	CATCTCAGCAGCAGTGTCTCTAC^{r}
RORγt forward	TGGGCATGTCCCGAGATG
RORγt reverse	GCAGGCTGTCCCTCTGCTT
STAT-3 forward	GGAGGAGGCATTCGGAAAGT
STAT-3 reverse	GCGCTACCTGGGTCAGCTT
FOXP3 forward	GAGAAGCTGAGTGCCATGCA
FOXP3 reverse	GCCACAGATGAAGCCTTGGT

IL, interleukin; *IFNG*, interferon γ; *FOXP3*, forkhead box protein 3; *GM-CSF*, granulocyte–macrophage colony-stimulating factor; *RORγt*, retinoic acid receptor-related orphan receptor γ isoform t; *STAT*, signal transducer and activator of transcription.

transcribed and labelled using One-Cycle Target Labeling and Control Reagents as instructed by the manufacturer (Affymetrix, Santa Clara, CA). The labelled probes were hybridized to a Human Genome U133 Plus 2·0 Array (Affymetrix). The arrays were used in a single experiment and analysed with GENECHIP operating software 1.2 (Affymetrix). Background subtraction and normalization were performed using GENESPRING GX 7.3 software (Agilent Technologies, Santa Clara, CA). The signal intensity was pre-normalized based on the positive control genes (GAPDH and β-actin) for all measurements on that chip. To account for differences in detection efficiency between spots, the pre-normalized signal intensity of each gene was normalized to the median of pre-normalized measurements for that gene. The data were filtered as follows. (i) Genes that were scored as absent in all samples were eliminated. (ii) Genes with a signal intensity of < 90 were eliminated. (iii) Genes that exhibited increased (fold-change > 2) or decreased (fold-change > 2) expression in CB-derived $CD4^+$ T cells compared with PB-derived $CD4^+$ T cells were selected by comparing the mean value of signal intensities in each condition.

Immunofluorescence study

After periods of cultivation, cells were collected and stained with fluorescence-labelled monoclonal antibodies and analysed by flow cytometry (FC500; Beckman/Coulter, Fullerton, CA). A four-colour immunofluorescence study was performed with a combination of fluorescein isothiocyanate (FITC)-conjugated anti-CD3, phycoerythrin (PE)-conjugated anti- forkhead box protein 3 (Foxp3), phycoerythrin-cyanine-5 (PC5)-conjugated anti-CD4 and PC7-conjugated anti-CD8 (Beckman/Coulter). After staining of cell surface antigens, cells were permeabilized with IntraPrep (Dako, Glostrup, Denmark) and intracellular antigen (Foxp3) was further stained.

Statistical analysis

The statistical analysis was performed using a Student's *t*-test and a *P*-value < 0·05 was considered to be statistically significant.

Results

Expression profiles of activated $CD4^+$ T cells derived from human CB and PB

To compare the gene expression patterns of CB-derived $CD4^+$ cells and PB-derived $CD4^+$ cells, we performed DNA microarray analysis using the Affymetrix Human Genome U133 Plus 2·0 Array. After background subtraction, comparison of the gene expression profiles of two independent CB-derived $CD4^+$ samples and PB-derived $CD4^+$ samples was performed using a gene cluster analysis. The genes differentially expressed (fold-change > 2) between the activated $CD4^+$ T cells derived from CB and those derived from PB were selected, and 396 probes were found to exhibit higher levels of expression in CB-derived $CD4^+$ samples while 131 probes exhibited higher levels in PB-derived $CD4^+$ samples. Parts of the data are summarized and presented in Fig. 1a and Tables 2–4.

Among these genes, those closely correlated to T-cell function and development were selected (Fig. 1b). The genes exhibiting higher levels of expression in CB-derived $CD4^+$ samples included those encoding cell cycle regulators, including cyclin-dependent kinase (CDKN)2A and 2B, transcriptional regulators and signal transduction factors (Tables 2 and 3). The genes for cytokines, chemokines and their receptors such as Interferon γ (IFNG), granulocyte-macrophage colony-stimulating factor (GM-CSF) and for T-cell transcriptional regulators (*FOXP3*) as well as the genes related to T-cell development including CD28, cytotoxic T lymphocyte antigen-4 (CTLA4) and inducible T-cell co-stimulator (ICOS) were also found among the genes exhibiting higher levels of expression in CB-derived $CD4^+$ samples (Fig. 1b). The factors reported

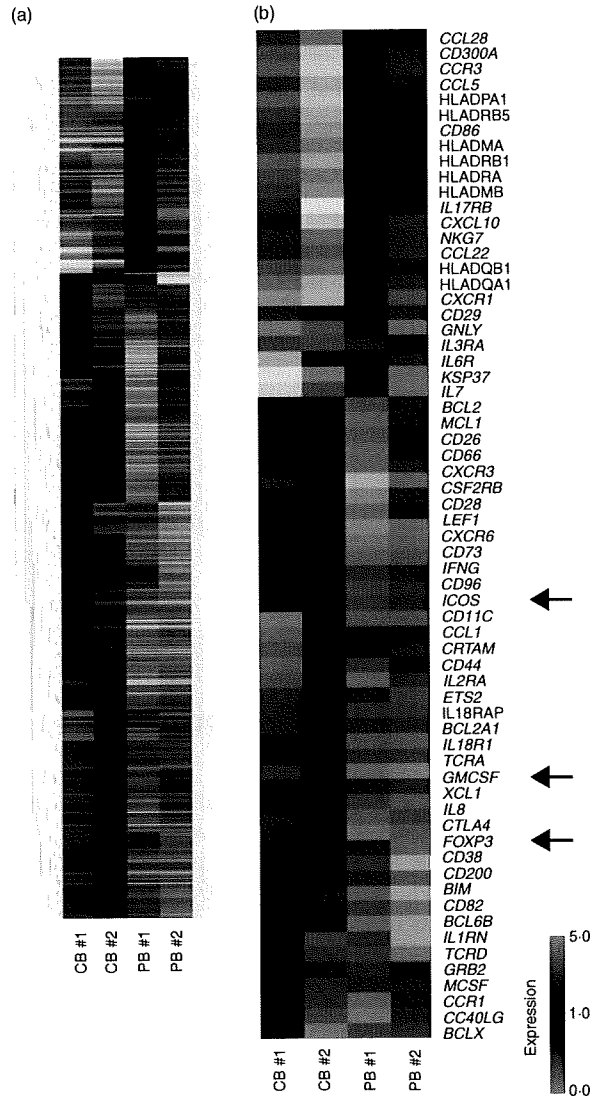

Figure 1. Comparison of the gene expression profiles of cord blood (CB)- and peripheral blood (PB)-derived $CD4^+$ T cells. Hierarchical clustering of results from a microarray analysis for CB- and PB-derived $CD4^+$ T cells is indicated. (a) A total of 529 genes characterizing $CD4^+$ T cells (396 genes for CB-derived $CD4^+$ T cells and 131 genes for PB-derived $CD4^+$ T cells) were used to create the gene tree. The gene list is presented in Tables 3 and 4. (b) Genes related to T-cell development (40 genes for CB-derived $CD4^+$ T cells and 26 genes for PB-derived $CD4^+$ T cells) are presented. The arrows indicate the expression pattern of T-cell lineage-specific genes including inducible T-cell co-stimulator (*ICOS*), granulocyte-macrophage colony-stimulating factor (*GM-CSF*) and forkhead box protein 3 (*FOXP3*).

to be essential for negative selection in $CD4^+$ $CD8^+$ thymocytes such as BCL2-like 11 (BIM)[10] as well as other apoptotic regulators were also found among the genes exhibiting higher expression levels in CB-derived $CD4^+$ samples.

The genes with a higher level of expression in the PB-derived $CD4^+$ T cells included those encoding transcriptional regulators, signal transduction factors, major histocompatibility complex (MHC) class II molecules (*HLADMA*, *HLADMB*, *HLADPA1*, *HLADQB1*, *HLADRA*, *HLADRB1* and *HLADRB5*), and cytokines, chemokines and their receptors (*IL-7*, *IL-17RB*), as well as genes that characterize the T-cell lineage (*CD29*, *CD86*) (Fig. 1b, Tables 2, 4).

Notably, microarray studies showed that the expression of several regulatory T cell (Treg)-related genes was significantly higher in the CB-derived T cells. Foxp3 is an important T-cell transcription factor and is considered to be a marker of Tregs. Cytotoxic T-lymphocyte antigen-4 (CTLA-4) and ICOS, which belong to the CD28 family of receptors and play a crucial role in the activation of T cells, were reported to be highly expressed in activated Tregs.[11,12] All of the above genes were expressed at higher levels in the CB-derived CD4 T cells (Fig. 1).

The microarray results for major genes related to the development of the T-cell lineage, including those not appeared in Fig. 1, are summarized in Table 2. As shown in Table 2, the expression of T-cell lineage master regulator genes, such as *TBX21*, *GATA3* and *MAF*, and T cell-related cytokines, such as *IL-4*, *IL-5*, *IL-13*, *IL-22* and *TGFB1*, revealed no significant difference between CB-derived $CD4^+$ cells and PB-derived $CD4^+$ cells. However, other T cell-related genes, including *IL-2*, *IL-6*, *IL-9*, *IL-10* and *IL-17*, were eliminated from the list in the course of background subtraction because the signal intensity of each gene was low (< 90 as raw data) in all of the samples.

Differences in the expression patterns of T-cell lineage-specific genes between CB-derived and PB-derived $CD4^+$ T cells

To further confirm the characteristic gene expression in CB- and PB-derived $CD4^+$ T cells, we performed a real-time RT-PCR analysis. Consistent with the microarray data, when the mRNA levels of the genes related to the T helper type 1 (Th1) and Th2 phenotypes were examined, higher levels of GM-CSF and IFNG were observed in CB-derived T cells, while IL-4 revealed no significant tendency (Fig. 2). We also examined IL-6 and IL-10 and no significant tendency was observed either in the expression of these genes (Fig. 2).

Next we examined the expression of the genes related to Tregs and observed a higher level of Foxp3, but lower levels of retinoic acid receptor-related orphan receptor γ isoform t (RORγt); and IL-17F, in CB-derived T cells (Fig. 3). In contrast, there was no significant tendency in the expression of genes encoding signal transducer and activator of transcription 3 (STAT-3), IL-23 and IL-23 receptors. In the case of the *IL-17* gene, clear amplifica-

Table 2. The microarray results for T-cell-related genes

			CB-1		CB-2		PB-1		PB-2	
Description	Gene	Gene ID	Normalized	Raw	Normalized	Raw	Normalized	Raw	Normalized	Raw
Master regulation										
Thl	*TBX21*	220684_at	1·1382915	305·7	0·7851455	247·1	1·045663	230·5	0·954337	261·4
Th2	*GATA3*	209602_s_at	1·471558	1204	0·7742825	742·1	1·0740323	721·1	0·9259675	772·5
	GATA3	209603_at	1·265932	416·5	0·53335179	205·7	1·0535141	284·5	0·9464856	317·6
	GATA3	209604_s_at	1·350573	5300	0·6415387	2950	1·0573606	3406	0·9426395	3773
	MAF	206363_at	0·7447395	672·7	0·8744312	925·6	1·1255689	834·5	1·2704437	1170
	MAF	209348_s_at	1·0320604	2078	0·8329663	1965	0·9679398	1600	1·8301903	3758
	MAF	229327_s_at	0·9099149	569·7	0·6089576	446·8	1·090085	560·2	1·4076804	898·9
Treg	*FOXP3*	221334_s_at	1·8893701	100·6	1·4199468	88·6	0·4988136	21·8	0·5800531	31·5
	FOXP3	224211_at	1·6205869	152·3	1·4101433	155·3	0·5898568	45·5	0·2347433	22·5
Cytokines										
Thl	*IFNG*	210354_at	1·4801383	2000	1·9182948	3037	0·457517	507·4	0·5198616	716·4
	GM-CSF	210229_s_at	1·2802086	1293	2·6726868	3163	0·6906437	572·5	0·7197912	741·4
Th2	*IL-4*	207538_at	2·0291064	687·2	0·3361219	133·4	0·9317174	259	1·0682826	369
	IL-4	207539_s_at	2·8263247	965	0·3561467	142·5	0·8481774	237·7	1·1518226	401·1
	IL-5	207952__at	1·3380713	810	0·0610382	43·3	1·0097023	501·7	0·9902797	611·4
	IL-13	207844_at	3·9835246	1712	0·8117443	408·8	1·1453367	404	0·8691162	452·9
Treg	*TGFB1*	203085_s_at	1·5166419	774·9	0·9012154	539·6	1·0987847	460·8	0·8546632	374·6
Others	*IL-22*	222974_at	0·1272062	5·2	4·325279	207·2	0·5632869	18·9	1·4367131	59·9
Surface molecules										
Treg	*CTLA4*	231794_at	1·3871489	336·9	1·2560804	357·5	0·7439196	148·3	0·4444751	110·1
	CTLA4	236341_at	1·2573498	905·7	1·6210791	1368	0·6800935	402·1	0·7426501	545·6
Others	*IL-2RA*	206341_at	1·5216751	3569	1·2715347	3494	0·7284654	1402	0·6569936	1571
	IL-2RA	211269_s_at	1·1563299	4436	1·3173387	5923	0·8436702	2657	0·560745	2194
	ICOS	210439_at	1·378036	619·8	1·343834	708·3	0·567216	209·4	0·656166	301
	CD28	211856_x_at	1·3887135	144·9	1·2905376	157·8	0·3292731	28·2	0·7094624	75·5
	CD28	211861_x_at	1·350062	183·3	1·4109998	224·5	0·4863549	54·2	0·649938	90

The microarray results for major genes related to the development of the T-cell lineage are summarized. The normalized and raw data for four samples are indicated for each gene. Those for which differential expression was found between cord blood (CB)- and peripheral blood (PB)-derived $CD4^+$ T cells in a gene cluster analysis (fold-change > 2) are highlighted in grey. Genes exhibiting low signal intensity (< 90 as raw data) in all of the four samples were eliminated from the list beforehand in the process of background subtraction, and thus do not appeared in this table.

CTLA-4, cytotoxic T-lymphocyte antigen-4; *FOXP3*, forkhead box protein 3; GATA, GATA family of zinc finger trancription factors; *GM-CSF*, granulocyte–macrophage colony-stimulating factor; ICOS, inducible T-cell co-stimulator; IFNG, interferon γ; *IL*, interleukin; MAF, macrophage-activating factor; TBX21, T-box protein 21; TGFB1, transforming growth factor, beta 1; Th1, T helper type 1; Treg, regulatory T cell.

tion was detected in PB-derived T cells whereas no amplification was observed in the samples of CB-derived T cells (data not shown).

To further investigate whether increased expression of the *FOXP3* gene is a general feature of CB-derived $CD4^+$ T cells, we tested four samples of CB-derived $CD4^+$ T cells by real-time RT-PCR analysis and compared the results with those for equivalent numbers of PB-derived samples. As shown in Fig. 4, two CB-derived samples (CB 4 and 5, at 2 weeks) revealed significantly increased gene expression of *FOXP3* when compared with PB-derived samples, whereas the remaining two samples (CB 3 and 6; termed 'additional' samples below) did not. We also tested *FOXP3* gene expression at an earlier time-point in the same samples and observed no significant increase of *FOXP3* gene expression in CB-derived $CD4^+$ T cells at 1 week (Fig. 4). When the data were analysed statistically, expression of the *FOXP3* gene was found to be significantly higher in CB-derived $CD4^+$ T cells in comparison with equivalent PB-derived $CD4^+$ T cells at both 1 week ($P < 0{\cdot}05$) and 2 weeks ($P < 0{\cdot}05$) (Fig. 4).

Next we assessed the expression of the Foxp3 protein in CB-derived $CD4^+$ T cells. When the same samples as described above were examined by flow cytometry using a specific antibody, the Foxp3 protein was certainly detected in a portion of cells in all of four CB-derived samples while not detected in any of the PB-derived samples tested (Fig. 5). Inconsistent with the results of real-time RT-PCR, expression level of Foxp3 proteins was higher in CB-derived $CD4^+$ T cells at 1 week than at 2 weeks.

Table 3. Genes up-regulated in $CD4^+$ T cells from cord blood samples 1 and 2 (CB 1 and CB 2, respectively)

		Fold change				
Affi ID	Gene abbreviation	CB 1	CB 2	PB 1	PB 2	Gene name
Apoptosis						
1555372_at	*BimL*	1·39	1·52	0·61	0·42	BCL2-like 11 (apoptosis facilitator)
237837_at	*BCL2*	1·27	1·32	0·49	0·73	B-cell CLL/lymphoma 2
205681_at	*BCL2A1*	1·91	1·53	0·39	0·47	BCL2-related protein A1
1558143_a_at	*BCL2L11*	1·68	1·74	0·32	0·32	BGL2-like 11 (apoptosis facilitator)
228311_at	*BCL6B*	1·36	3·39	0·64	0·26	B-cell CLL/lymphoma 6, member B (zinc finger protein)
215037_s_at	*BCLX*	2·56	1·27	0·73	0·56	BCL2-like 1
224414_s_at	*CARD6*	2·65	1·34	0·56	0·66	Caspase recruitment domain family, member 6
201631_s_at	*IER3*	1·62	2·95	0·38	0·31	Immediate early response 3
218000_s_at	*PHLDA1*	2·34	1·21	0·53	0·79	Pleckstrin homology-like domain, family A, member 1
209803_s_at	*PHLDA2*	2·87	1·32	0·31	0·68	Pleckstrin homology-like domain, family A. member 2
203063_at	*PPMIF*	1·26	1·53	0·74	0·64	Protein phosphatase IF (PP2C domain containing)
205214_at	*STK17B*	1·78	1·26	0·74	0·71	Serine/threonine kinase 17b (apoptosis-inducing)
217853_at	*TENS1*	1·63	6·00	0·04	0·37	Tensin 1
B- and T-cell development						
211861_x_at	*CD28*	1·35	1·41	0·49	0·65	CD28 antigen(Tp44)
207892_at	*CD40LG*	3·67	1·32	0·45	0·68	C040 ligand (TNF superfamily, member 5, hyper-IgM syndrome)
206914_at	*CRTAM*	2·76	1·60	0·40	0·36	Class I MHC-restricted T-cell-associated molecule
210557_x_at	*CSF1*	3·79	1·22	0·78	0·70	Colony-stimulating factor 1 (macrophage)
210229_s_at	*CSF2*	1·28	2·67	0·69	0·72	Colony-stimulating factor 2 (granulocyte–macrophage)
205159_at	*CSF2RB*	2·33	1·60	0·18	0·40	Colony-stimulating factor 2 receptor
231794_at	*CTLA4*	1·39	1·26	0·74	0·44	Cytotoxic T-lymphocyte-associated protein 4
204232_at	*FCER1G*	1·63	2·14	0·28	0·37	Fc fragment of IgE, high affinity 1, receptor for; gamma polypeptide
210439_at	*ICOS*	1·38	1·34	0·57	0·66	Inducible T-cell costimulator
210354_at	*IFNG*	1·48	1·92	0·46	0·52	Human mRNA for HuIFN -gamma interferon
230536_at	*PBX4*	1·48	1·26	0·50	0·74	Pre-B-cell leukaemia transcription factor 4
215540_at	*TCRA*	1·25	1·87	0·67	0·75	T-cell antigen receptor alpha
234440_al	*TCRD*	7·51	1·48	0·50	0·52	Human T-cell receptor delta-chain
Cell growth and maintenance						
213497_at	*ABTB2*	2·06	1·34	0·66	0·63	Ankyrin repeat and BTB (POZ) domain containing 2
201236_s_at	*BTG2*	1·60	1·23	0·60	0·77	BTG family, member 2
235287_at	*CDK6*	1·50	1·32	0·44	0·68	Cyclin-dependent kinase 6
209644_x_at	*CDKN2A*	2·90	1·21	0·67	0·79	Cyclin-dependent kinase inhibitor 2A (melanoma, p16, inhibits CDK4)
236313_at	*CDKN2B*	3·24	1·28	0·58	0·72	Cyclin-dependent kinase inhibitor 2B (p15, inhibits CDK4)
241984_at	*CHES1*	1·38	1·34	0·66	0·63	Checkpoint suppressor 1
202552_s_at	CRIM1	1·94	1·39	0·32	0·61	Cysteine-rich transmembrane BMP regulator 1 (chordin-like)
204844_at	*ENPEP*	1·64	1·75	0·09	0·36	Glutamyl aminopeptidase (aminopeptidase A)
205418_at	*FES*	1·39	1·80	0·61	0·25	Feline sarcoma oncogene
228572_at	*GRB2*	4·69	1·21	0·79	0·78	Growth factor receptor-bound protein 2
207688_s_at	*INHBC*	1·46	1·25	0·51	0·75	Inhibin, beta C
209744_x_at	*ITCH*	1·30	1·47	0·63	0·70	Itchy homolog E3 ubiquitin protein ligase (mouse)
201548_s_at	*JARID1B*	1·27	1·92	0·73	0·46	Jumonji, AT-rich interactive domain IB (RBP2-like)
203297_s_at	*JARID2*	1·42	1·28	0·54	0·72	Jumonji, AT-rich interactive domain 2
41387_r_at	*JMJD3*	1·82	1·24	0·76	0·65	Jumonji domain containing 3
205569_at	*LAMP3*	2·32	1·24	0·76	0·50	Lysosomal-associated membrane protein 3
214039_s_at	*LAPTM4B*	1·41	1·49	0·49	0·59	Lysosomal-associated protein transmembrane 4 beta
205857_x_at	*MSH3*	1·79	1·28	0·58	0·72	MutS homolog 3 (*E. coli*)
209550_at	*NDN*	3·42	1·38	0·17	0·62	Necdin homolog (mouse)
207943_x_at	*PLAGL1*	1·37	1·43	0·57	0·63	Pleiomorphic adenoma gene-like 1
204748_at	*PTGS2*	1·65	1·78	0·14	0·35	Prostaglandin-endoperoxide synthase 2
201482_at	*QSCN6*	1·32	1·23	0·38	0·77	Quiescin Q6
203743_s_at	*TDG*	1·47	1·23	0·54	0·77	Thymine-DNA glycosylase
204227_s_at	*TK2*	2·12	1·26	0·56	0·74	Thymidine kinase 2, mitochondrial

Table 3. Continued

Affi ID	Gene abbreviation	Fold change CB 1	CB 2	PB 1	PB 2	Gene name
Cytokines and chemokines						
207533_at	*CCL1*	1·67	1·48	0·52	0·49	Chemokine (C-C motif) ligand 1
205099_s_at	*CCR1*	4·70	1·21	0·61	0·79	Chemokine (C-C motif) receptor 1
207681_at	*CXCR3*	1·51	1·33	0·41	0·67	Chemokine (C-X-C motif) receptor 3
211469_s_at	*CXCR6*	1·58	1·95	0·32	0·42	Chemokine (C-X-C motif) receptor 6
206613_at	*IL-18R1*	2·32	1·38	0·61	0·62	Interleukin-18 receptor 1
207072_at	*IL-18RAP*	2·16	1·44	0·46	0·56	Interleukin-18 receptor accessory protein
212657_s_at	*IL-1RN*	1·44	3·12	0·56	0·37	Interleukin 1 receptor
206341_at	*IL-2RA*	1·52	1·27	0·73	0·66	Interleukin-2 receptor alpha
202859_x_at	*IL-8*	1·31	3·75	0·38	0·69	Interleukin-8
202643_s_at	*TNFAIP3*	1·61	1·25	0·67	0·75	Tumour necrosis factor, alpha-induced protein 3
202687_s_at	*TNFSF10*	2·83	1·23	0·67	0·77	Tumour necrosis factor (ligand) superfamily member 10
205599_at	*TRAF1*	2·25	1·32	0·68	0·61	Tumour necrosis factor receptor-associated factor 1
202871_at	*TRAF4*	1·43	1·58	0·57	0·48	Tumour necrosis factor receptor-associated factor 4
206366_x_at	*XCL1*	1·24	2·66	0·46	0·76	Chemokine (C motif) ligand 1
Signal transduction						
210538_s_at	*AIP1*	1·35	1·54	0·65	0·61	Baculoviral IAP repeat-containing 3
209369_at	*ANXA3*	1·39	6·82	0·61	0·05	Annexin A3
1554343_a_at	*BRDG1*	1·45	1·67	0·52	0·55	BCR downstream signalling 1
225946_at	*C12orf2*	3·20	1·77	0·23	0·23	Ras association (RaIGDS/AF-6) domain family 8
204392_at	*CAMK1*	1·26	1·62	0·74	0·54	Calcium/calmodulin-dependent protein kinase I
231042_s_at	*CAMK2D*	1·31	1·63	0·25	0·69	Calcium/calmodulin-dependent protein kinase (CaM kinase) II delta
205692_s_at	*CD38*	1·37	1·29	0·71	0·48	CD38 antigen (p45)
231747_at	*CYSLTR1*	3·16	1·45	0·55	0·43	Cysteinyl leukotriene receptor 1
211272_s_at	*DGKA*	1·43	1·23	0·77	0·54	Diacylglycerol kinase alpha 80 kDa
200762_at	*DPYSL2*	1·35	1·40	0·37	0·65	Dihydropyrimtdinase-like 2
208370_s_at	*DSCR1*	1·23	1·90	0·63	0·77	Down syndrome critical region gene 1
204794_at	*DUSP2*	1·55	2·57	0·39	0·45	Dual specificity phosphatase 2
204015_s_at	*DUSP4*	1·35	2·66	0·65	0·39	Dual specificity phosphatase 4
211333_s_at	*FASLG*	1·20	1·37	0·49	0·80	Fas ligand (TNF superfamily, member 6)
211535_s_at	*FGFR1*	1·23	2·79	0·70	0·77	Fibroblast growth factor receptor 1
224148_at	*FYB*	1·50	1·21	0·45	0·79	FYN binding protein (FYB-120/130)
209304_x_at	*GADD45B*	1·55	1·29	0·65	0·71	Growth arrest and DNA-damage-inducible beta
234284_at	*GNG8*	1·50	3·16	0·50	0·35	Guanine nucleotide binding protein (G protein), gamma 8
224285_at	*GPR174*	1·91	1·42	0·56	0·58	G protein-coupled receptor 174
223767_at	*GPR84*	4·41	1·44	0·05	0·56	G protein-coupled receptor 84
211555_s_at	*GUCY1B3*	1·66	1·73	0·34	0·03	Guanylate cyclase 1, soluble, beta 3
38037_at	*HBEGF*	1·54	1·36	0·55	0·64	Heparin-binding EGF-like growth factor
203820_s_at	*IMP-3*	1·83	2·18	0·17	0·17	IGF-II-mRNA-binding protein 3
203006_at	*INPP5A*	1·40	1·86	0·60	0·52	Inositol polyphosphate-5-phosphatase, 40 kDa
231779_at	*IRAK2*	1·93	1·46	0·46	0·54	Interleukin-1 receptor associated kinase 2
32137_at	*JAG2*	1·58	1·29	0·71	0·64	Jagged 2
203904_x_at	*KAI1*	1·65	1·59	0·41	0·25	CD82 antigen
235252_at	*KSR*	1·72	1·56	0·43	0·44	Kinase suppressor of ras 1
210948_s_at	*LEF1*	1·21	1·64	0·41	0·79	Hypothetical protein LOC641518
203236_s_at	*LGALS9*	1·48	1·27	0·73	0·51	Lectin, galactoside-binding, soluble, 9 (galectin 9)
220253_s_at	*LRP12*	1·27	1·30	0·31	0·73	Low-density lipoprotein-related protein 12
206637_at	*P2RY14*	1·32	1·48	0·39	0·68	Purinergic receptor P2Y, G-protein coupled, 14
210837_s_at	*PDE4D*	1·35	1·31	0·62	0·69	Phosphodiesterase 4D, cAMP-specific
206726_at	*PGDS*	6·45	1·40	0·60	0·43	Prostaglandin D2 synthase, haematopoietic
210617_at	*PHEX*	1·53	4·08	0·21	0·47	Phosphate regulating endopeptidase homologue, X-linked
206370_at	*PIK3CG*	1·23	1·32	0·50	0·77	Phosphoinositide-3-kinase, catalytic, gamma polypeptide
205632_s_at	*PIP5K1B*	1·32	1·42	0·64	0·68	Phosphalidylinositol-4-phosphate 5-kinase, type 1 beta

Table 3. Continued

Affi ID	Gene abbreviation	Fold change CB 1	CB 2	PB 1	PB 2	Gene name
215195_at	*PRKCA*	2·17	1·36	0·64	0·61	Protein kinase C, alpha
210832_x_at	*PTGER3*	4·44	1·47	0·07	0·53	Prostaglandin E receptor 3 (subtype EP3)
1553535_a_at	*RANGAP1*	1·58	1·39	0·58	0·61	Ran GTPase activating protein 1
234344_at	*RAP2C*	1·75	1·26	0·46	0·74	RAP2C, member of RAS oncogene family
223809_at	*RGS18*	2·12	1·67	0·15	0·33	Regulator of G-protein signalling 18
209882_at	*RIT1*	1·74	1·32	0·63	0·68	Ras-like without CAAX 1
209451_at	*TANK*	1·34	1·20	0·42	0·80	TRAF family member-associated NFKB activator
204924_at	*TLR2*	1·60	2·52	0·36	0·40	Toll-like receptor 2
217979_at	*TM4SF13*	1·21	2·47	0·30	0·79	Tetraspanin 13
209263_x_at	*TM4SF7*	2·05	1·41	0·58	0·59	Tetraspanin 4
Transcription						
1566989_at	*ARID1B*	1·42	1·27	0·09	0·73	AT-rich interactive domain 1B (SWIl-like)
203973_s_at	*CEBPD*	3·06	1·51	0·33	0·49	CCAAT/enhancer binding protein (C/EBP), delta
221598_s_at	*CRSP8*	1·60	1·29	0·71	0·68	Cofactor required for Spl transcriptional activation, subunit 8, 34 kDa
205249_at	*EGR2*	1·33	4·27	0·67	0·60	Early growth response 2 (Krox-20 homologue, *Drosophila*)
206115_at	*EGR3*	1·31	6·15	0·69	0·48	Early growth response 3
201328_at	*ETS2*	1·57	1·72	0·43	0·40	V-ets erythroblastosis virus E26 oncogene homologue 2 (avian)
218810_at	*FLJ23231*	2·13	1·37	0·63	0·63	Zinc finger CCCH-type containing 12A
209189_at	*FOS*	21·56	1·31	0·13	0·69	V-fos FBJ murine osteosarcoma viral oncogene homologue
223408_s_at	*FOXK2*	2·26	1·22	0·48	0·78	Forkhead box K2
202723_s_at	*FOXO1A*	1·47	1·27	0·57	0·73	Forkhead box O1A (rhabdomyosarcoma)
224211_at	*FOXP3*	1·62	1·41	0·59	0·23	Forkhead box P3
207156_at	*HIST1H2AG*	1·73	1·30	0·41	0·70	Histone 1, H2ag
220042_x_at	*HIVEP3*	1·26	1·65	0·74	0·56	Human immunodeficiency virus type I enhancer binding protein 3
207826_s_at	*ID3*	1·34	8·64	0·60	0·66	Inhibitor of DNA binding 3, dominant negative helix-loop-hetix protein
204549_at	*IKBKE*	2·33	1·29	0·71	0·66	Inhibitor of kappa light polypeptide gene enhancer in B cells
219878_s_at	*KLF13*	1·89	1·26	0·34	0·74	Kruppel-like factor 13
207667_s_at	*MAP2K3*	1·33	1·28	0·72	0·57	Mitogen-activated protein kinase kinase 3
201502_s_at	*NFKBIA*	2·31	1·29	0·71	0·57	Nuclear factor of κ light polypeptide gene enhancer in B cells inhibitor
222105_s_at	*NKIRAS2*	1·84	1·21	0·69	0·79	NFKB inhibitor interacting Ras-like 2
204622_x_at	*NR4A2*	1·35	4·31	0·65	0·63	Nuclear receptor subfamily 4, group A, member 2
207978_s_at	*NR4A3*	1·33	3·53	0·62	0·67	Nuclear receptor subfamily 4, group A, member 3
202600_s_at	*NRIPI*	1·86	1·39	0·26	0·61	Nuclear receptor interacting protein 1
216841_s_at	*SOD2*	1·25	1·73	0·36	0·75	Superoxide dismutase 2, mitochondrial
201416_at	*SOX4*	1·53	2·21	0·47	0·38	SRY (sex determining region Y)-box 4
223635_s_at	*SSBP3*	2·12	1·25	0·75	0·62	Single-stranded DNA binding protein 3
206506_s_at	*SUPT3H*	1·47	1·31	0·57	0·69	Suppressor of Ty 3 homologue (*S. cerevisiae*)
221618_s_at	*TAF9L*	1·25	1·49	0·47	0·75	TAF9-like RNA polymerase II
203177_x_at	*TFAM*	1·63	1·23	0·77	0·57	Transcription factor A, mitochondrial
213943_at	*TWIST1*	1·89	3·14	0·04	0·11	Twist homologue 1 (acrocephalosyndactyly 3; Saethre-Chotzen syndrome)
219836_at	*ZBED2*	1·33	4·76	0·67	0·21	Zinc finger, BED-type containing 2
211965_at	*ZFP36L1*	2·02	1·47	0·29	0·53	Zinc finger protein 36, C3H type-like 1
230760_at	*ZFY*	1·41	1·25	0·75	0·02	Zinc finger protein, Y-linked
228854_at	*ZNF145*	3·26	1·21	0·40	0·79	Transcribed locus
235121_at	*ZNF542*	2·68	1·33	0·63	0·67	Zinc finger protein 542

To investigate whether increased expression of the *IL-17* gene is a general feature of PB-derived $CD4^+$ T cells, we also tested *IL-17* gene expression in the above-described additional samples by real-time RT-PCR analysis. As shown in Fig. 6, all of four PB-derived $CD4^+$ T-cell samples revealed significantly increased gene expression of *IL-17* when compared with the CB-derived samples at 1 week. At 2 weeks, however, *IL-17* gene expression in PB-derived $CD4^+$ T cells was diminished while some of the CB-derived $CD4^+$ T cells (such as sample CB 4) exhibited increased *IL-17* gene expression. When the data were analysed statistically, expression of the *IL-17* gene was found to be

Table 4. Genes up-regulated in $CD4^+$ T cells from peripheral blood (PB)

Affi ID	Gene abbreviation	Fold change CB 1	CB 2	PB 1	PB 2	Gene name
Apoptosis						
1553681_a_at	*PRF1*	0·66	0·51	1·41	1·34	Perforin 1 (pore-forming protein)
B- and T-cell development						
224499_s_at	*AICDA*	0·06	0·44	1·56	3·47	Activation-induced cytidine deaminase
205495_s_at	*GNLY*	0·40	0·51	1·49	6·34	Granulysin
217478_s_at	*HLA-DMA*	0·67	0·39	1·33	1·35	Major histocompatibility complex, class II, DM alpha
203932_at	*HLA-DMB*	0·64	0·31	2·02	1·36	Major histocompatibility complex, class II, DM beta
211991_s_at	*HLA-DPA1*	0·50	0·14	1·54	1·50	Major histocompatibility complex, class II, DP alpha 1
212671_s_at	*HLA-DQA1*	0·44	0·23	1·56	2·56	Major histocompatibility complex, class II, DQ alpha 1
211656_x_at	*HLA-DQB1*	0·63	0·48	1·37	7·07	Major histocompatibility complex, class II, DQ beta 1
210982_s_at	*HLA-DRA*	0·58	0·37	1·50	1·42	Major histocompatibility complex, class II, DR alpha
208306_x_at	*HLA-DRB1*	0·51	0·24	1·49	1·61	Major histocompatibility complex, class II, DR beta 3
204670_x_at	*HLA-DRB5*	0·63	0·22	1·47	1·37	Major histocompatibility complex, class II, DR beta 5
211634_x_at	*IGHV1-69*	0·69	0·77	1·23	1·99	Immunoglobulin heavy variable 1–69
211645_x_at	*IgK*	0·15	0·49	1·51	6·62	Immunoglobulin kappa light chain (IGKV)
221651_x_at	*IGKC*	0·46	0·68	1·32	5·57	Immunoglobulin kappa constant
215379_x_at	*IGLC2*	0·62	0·41	1·38	4·26	Immunoglobulin lambda joining 2
209031_at	*IGSF4*	0·50	0·03	2·33	1·50	Immunoglobulin superfamily, member 4
205686_s_at	*CD86*	0·70	0·23	1·30	1·39	CD86 antigen (CD28 antigen ligand 2, B7-2 antigen)
204698_at	*ISG20*	0·68	0·49	1·32	1·64	Interferon stimulated exonuclease gene, 20 kDa
213915_at	*NKG7*	0·72	0·42	1·28	2·31	Natural killer cell group 7 sequence
Cell growth and maintenance						
201334_s_at	*ARHGEF12*	0·74	0·50	1·26	1·96	Rho guanine nucleotide exchange factor (GEF) 12
230292_at	*CHC1L*	0·70	0·56	1·30	2·02	Regulator of chromosome condensation (RCC1)
205081_at	*CRIP1*	0·56	0·73	1·27	1·75	Cysteine-rich protein 1 (intestinal)
31874_at	*GAS2L1*	0·77	0·52	1·23	2·35	Growth arrest-specific 2 like 1
202364_at	*MXI1*	0·43	0·73	1·27	1·44	MAX interactor 1
219304_s_at	*PDGFD*	0·65	0·71	1·29	3·68	Platelet-derived growth factor D
213397_x_at	*RNASE4*	0·64	0·46	1·36	2·21	Ribonuclease, RNase A family, 4
213566_at	*RNASE6*	0·69	0·39	1·49	1·31	Ribonuclease, RNase A family, k6
219077_s_at	*WWOX*	0·40	0·78	1·25	1·22	WW domain containing oxidoreductase
Cytokine and chemokine						
207861_at	*CCL22*	0·76	0·52	1·24	2·47	Chemokine (C–C motif) ligand 22
238750_at	*CCL28*	0·74	0·45	1·26	1·41	Chemokine (C–C motif) ligand 28
1555759_a_at	*CCL5*	0·71	0·23	1·29	1·92	Chemokine (C–C motif) ligand 5
208304_at	*CCR3*	0·50	0·12	1·50	2·35	Chemokine (C–C motif) receptor 3
205898_at	*CX3CR1*	0·30	0·20	1·70	4·16	Chemokine (C–X3–C motif) receptor 1
204533_at	*CXCL10*	0·80	0·16	1·20	2·53	Chemokine (C–X–C motif) ligand 10
219255_x_at	*IL-17RB*	0·73	0·04	1·27	1·29	Interleukin 17 receptor B
206148_at	*IL-3RA*	0·60	0·54	2·46	1·40	Interleukin 3 receptor, alpha (low affnity)
226333_at	*IL-6R*	0·22	0·79	1·21	2·43	Interleukin-6 receptor
206693_at	*IL-7*	0·09	0·54	1·46	5·86	Interleukin-7
Signal transduction						
204497_at	*ADCY9*	0·76	0·40	1·24	2·40	Adenylate cyclase 9
206170_at	*ADRB2*	0·58	0·35	1·42	3·97	Adrenergic, beta-2-, receptor, surface
202096_s_at	*BZRP*	0·50	0·54	1·59	1·46	Benzodiazapine receptor (peripheral)
230464_at	*EDG8*	0·04	0·09	1·91	2·42	Endothelial differentiation, sphingolipid G-protein-coupled receptor 8
223423_at	*GPR160*	0·54	0·68	1·40	1·32	G protein-coupled receptor 160
227769_at	*GPR27*	0·07	0·08	1·92	244	G protein in-coupled receptor 27
210095_s_at	*IGFBP3*	0·27	0·20	1·73	5·25	Insulin-like growth factor binding protein 3
38671_at	*PLXND1*	0·08	0·65	1·35	2·57	Plexin D1
226101_at	*PRKCE*	0·56	0·43	1·72	1·44	Protein kinase C. epsilon
232629_at	*PROK2*	0·01	0·13	1·87	2·09	Prokineticin 2

Table 4. Continued

Affi ID	Gene abbreviation	Fold change CB 1	CB 2	PB 1	PB 2	Gene name
203329_at	*PTPRM*	0·36	0·62	1·38	1·93	Protein tyrosine phosphatase, receptor type, M
204731_at	*TGFBR3*	0·78	0·55	1·22	2·04	Transforming growth factor, beta receptor III (betaglycan, 300 kDa)
Transcription						
203129_s_at	*KIF5C*	0·67	0·09	1·33	3·43	Kinesin family member 5C
213906_at	*MYBL1*	0·75	0·51	1·25	3·63	V-myb myeloblastosis viral oncogene homologue (avian)-like 1
209815_at	*PTCH*	0·59	0·27	1·41	4·17	Patched homologue (*Drosophila*)
213891_s_at	*TCF4*	0·74	0·65	2·06	1·26	Transcription factor 4
238520_at	*TRERF1*	0·70	0·77	1·23	2·30	Transcriptional regulating factor 1
203603_s_at	*ZFHX1B*	0·74	0·61	1·26	3·63	Zinc finger homobox 1b
213218_at	*ZNF187*	0·74	0·69	1·26	1·76	Zinc finger protein 187
221123_x_at	*ZNF395*	0·38	0·71	1·63	1·29	Zinc finger protein 395

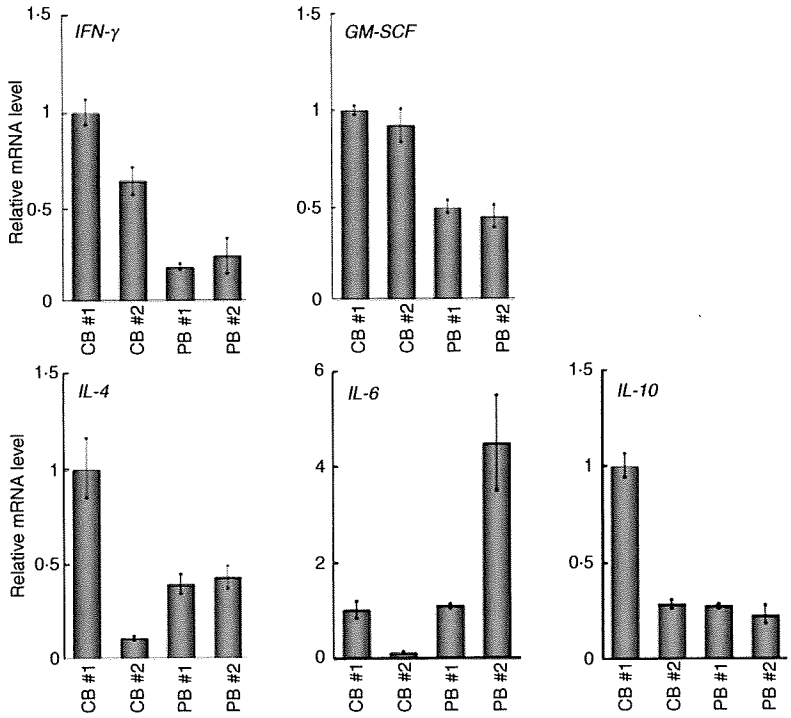

Figure 2. Quantitative polymerase chain reaction (PCR) analysis of the genes related to the T helper type 1 (Th1) and Th2 phenotypes. The expression of the genes indicated was examined by real-time reverse transcriptase (RT)-PCR using the same sample specimens as in Fig 1. Data are normalized to the mRNA level in PB 1 which is arbitrarily set to 1. The signal intensity was normalized using that of a control housekeeping gene [the human glyceraldehyde-3-phosphate dehydrogenase (*GAPDH*) gene]. Data are relative values with the standard deviation (SD) for triplicate wells.

significantly higher in PB-derived $CD4^+$ T cells in comparison with equivalent CB-derived $CD4^+$ T cells at 1 week ($P < 0{\cdot}05$) but not at 2 weeks (Fig. 6).

Discussion

Although it is generally believed that there are functional differences between CB and PB lymphocytes, the details are obscure. For instance, Azuma *et al.*[13] reported that the phenotype and function of expanded CB lymphocytes were essentially equivalent to those of expanded PB lymphocytes when evaluated in *in vitro* experiments. In the present study, however, we have shown that CB-derived $CD4^+$ T cells revealed a distinct expression profile of genes important for the function of particular T-cell subsets compared with PB-derived $CD4^+$ T cells.

$CD4^+$ T cells can be classified into distinct subsets, including effector $CD4^+$ cells and Tregs, according to their functional characteristics as well as differentiation profiles.[14–16] Typically, effector $CD4^+$ T cells have been further divided into two distinct lineages on the basis of their cytokine production profiles, namely Th1 and Th2. Th1 cells producing cytokines such as IL-2, IFN-γ and GM-CSF have evolved to enhance the eradication of intracellular pathogens and are thought to be potent activators of cell-mediated immunity. In contrast, Th2

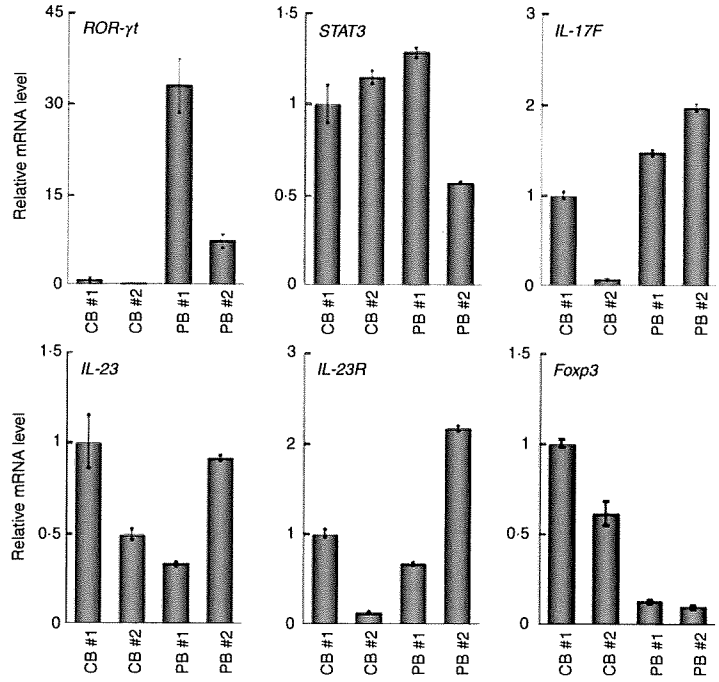

Figure 3. Quantitative polymerase chain reaction (PCR) analysis of the forkhead box protein 3 gene (*FOXP3*) and the genes related to the secretion of interleukin (IL)-17. The expression of the genes indicated was examined as in Fig 2. Data are normalized to the mRNA level in peripheral blood sample 1 (PB 1) as in Fig.2. The signal intensity was normalized using that of a control housekeeping gene [the human glyceraldehyde-3-phosphate dehydrogenase (*GAPDH*) gene]. Data are relative values with the standard deviation for triplicate wells.

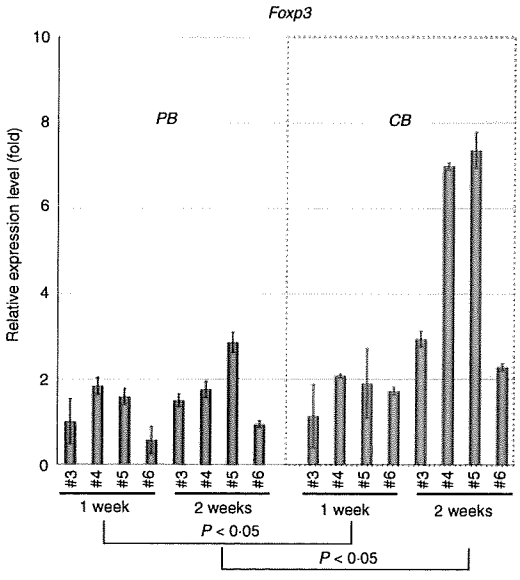

Figure 4. Quantitative polymerase chain reaction (PCR) analysis of the forkhead box protein 3 gene (*FOXP3*) in additional samples. Additional peripheral blood (PB) and cord blood (CB) samples were prepared and RNAs were extracted at 1 and 2 weeks. The expression of the *FOXP3* gene was examined as in Fig. 2. Data are normalized to the mRNA level in the sample of PB 3 at 1 week, which is arbitrarily set to 1. The signal intensity was normalized using that of a control housekeeping gene (the human β-actin gene). Data are relative values with the standard deviation for triplicate wells. The data were analysed statistically and *FOXP3* gene expression in CB-derived $CD4^+$ T cells was found to be significantly higher in comparison with equivalent PB-derived $CD4^+$ T cells at both 1 week ($P < 0{\cdot}05$) and 2 weeks ($P < 0{\cdot}05$).

cells secreting cytokines such as IL-4, IL-5, IL-6, IL-9 and IL-13 have evolved to enhance the elimination of parasitic infections and are thought to be potent activators of B-cell immunoglobulin E production, eosinophil recruitment, and mucosal expulsion. Th1-type responses to self or commensal floral antigens can promote tissue destruction and chronic inflammation, whereas dysregulated Th2-type responses can cause allergy and asthma. The development of Th1 is specified by the transcription factor T-bet (also known as Tbx-21) and master regulators of Th2 differentiation are GATA-3 and c-maf.

As shown in Fig. 2 and Table 2, the gene expression profiles of CB- and PB-derived $CD4^+$ T cells revealed no significant differences regarding cytokines related to the definition of Th1 and Th2, with the exceptions of IFN-γ and GM-CSF. The mRNA levels of IFN-γ and GM-CSF tended to be higher in CB-derived $CD4^+$ T cells than in PB-derived $CD4^+$ T cells. The mRNA expression of the transcription factors T-bet, GATA-3 and c-maf, which regulate Th1 and Th2 cell differentiation, did not differ significantly between CB- and PB-derived $CD4^+$ T cells.

In addition to Th1 and Th2 cells, IL-17 (also known as IL-17A)-producing T lymphocytes have been recently shown to comprise a distinct third subset of T helper cells, termed Th17 cells, in the mouse immune system. Th17 cells exhibit pro-inflammatory characteristics and act as major contributors to autoimmune disease. A number of experiments using animal models support a significant role for IL-17 in the response to allografts.[14,16,17] There is as yet no direct evidence for the existence of discrete Th17 cells in humans, although

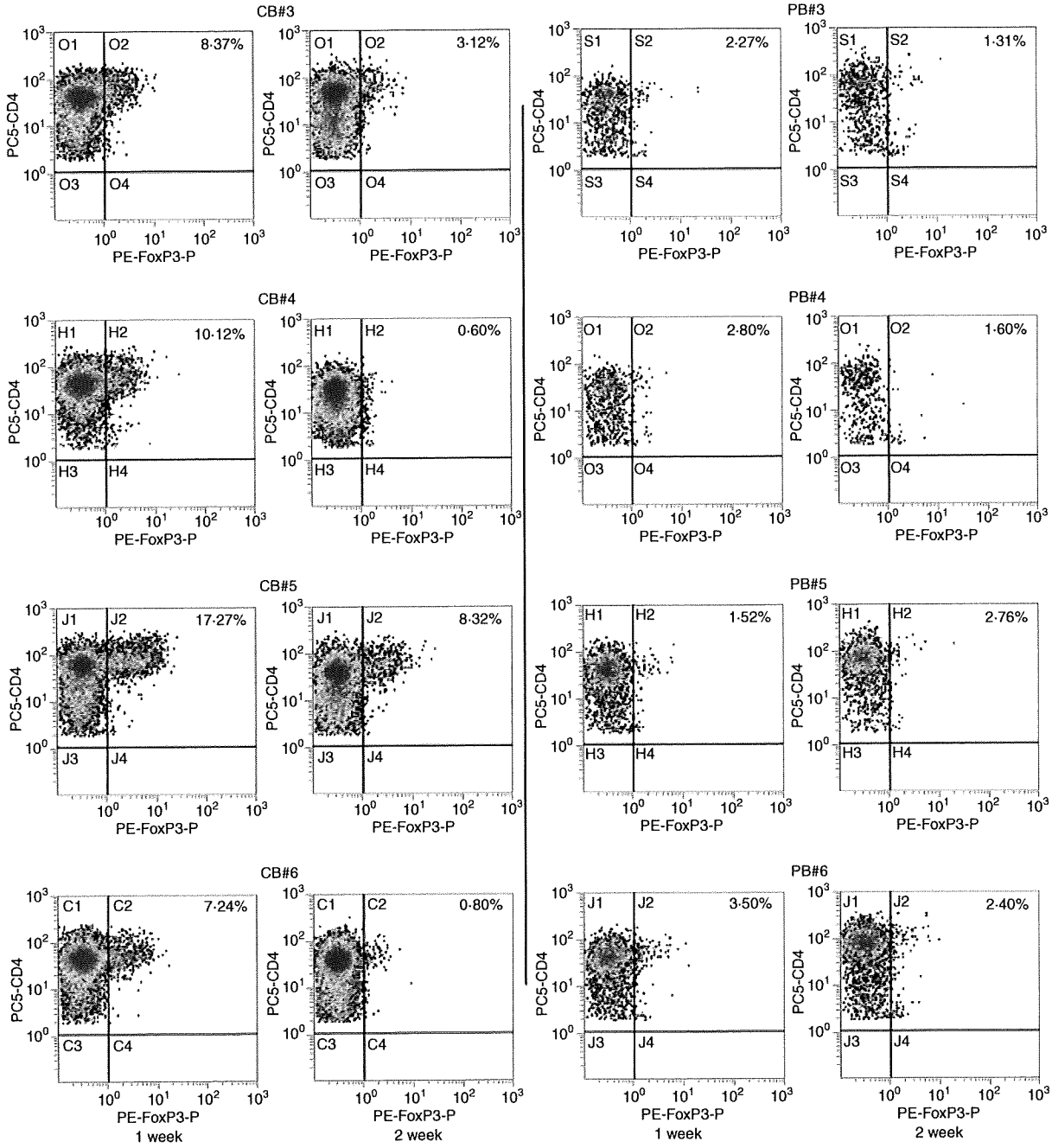

Figure 5. Protein expression of forkhead box protein 3 (Foxp3) in activated $CD4^+$ T cells. The protein expression of Foxp3 in same sample specimens as in Fig. 4 was examined by flow cytometry. The CD4 versus Foxp3 cytogram of the population gated with $CD3^+$ and $CD4^+$ in each sample is presented.

helper T cells secreting IL-17 have clearly been detected in the human immune system.[18] Several studies have shown a correlation between allograft rejection and IL-17. For example, IL-17 levels are elevated in human renal allografts during subclinical rejection and there are detectable mRNA levels in the urinary mononuclear cell sediments of these patients.[19,20] In human lung organ transplantation, IL-17 levels have also been reported to be elevated during acute rejection.[21] Interestingly, in this study, most of the PB-derived $CD4^+$ T-cell samples expressed higher levels of IL-17 mRNA than the CB-derived $CD4^+$ T-cell samples, suggesting that PB-derived $CD4^+$ T cells frequently include potent IL-17-secreting T cells.

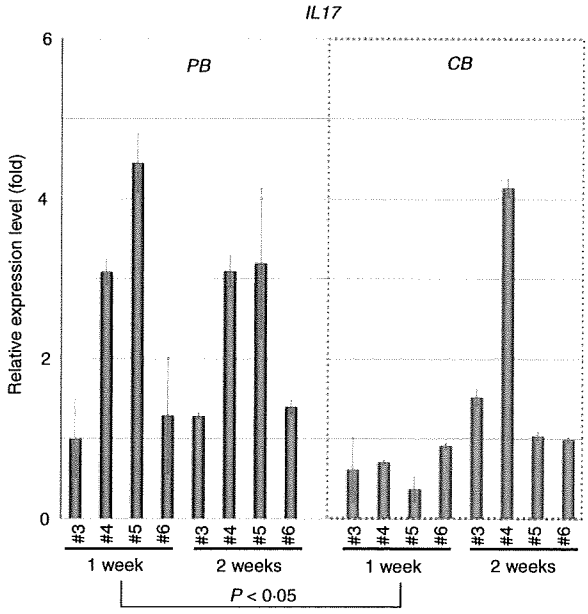

Figure 6. Quantitative polymerase chain reaction (PCR) analysis of interleukin (IL)-17 in additional samples. The expression of the *IL-17* gene in the same sample specimens as in Fig. 4 was examined and presented as in Fig 2. The data were analysed statistically and *IL-17* gene expression in peripheral blood (PB)-derived $CD4^+$ T cells was found to be significantly higher in comparison with equivalent CB-derived $CD4^+$ T cells at 1 week ($P < 0{\cdot}05$) but not at 2 weeks.

Th17 cells expand independently of T-bet or STAT-1. Ivanov *et al.*[22] have shown that the orphan nuclear receptor RORγt is the key transcription factor orchestrating the differentiation of the effector lineage. RORγt induces transcription of the gene encoding IL-17 in naïve $CD4^+$ T helper cells and is required for its expression in response to IL-6 and transforming growth factor (TGF)-β, the cytokines known to induce IL-17 expression. IL-23 is also involved in Th17 cell differentiation, but naïve T cells do not have the IL-23 receptor and are relatively refractory to IL-23 stimulation.[23,24] Although IL-23 seems to be an essential survival factor for Th17 cells, it is not required during their differentiation. It has been suggested that IL-23R expression is up-regulated on $ROR\gamma t^+$ Th17 cells in an IL-6-dependent manner. IL-23 may therefore function subsequent to IL-6/TGF-β-induced commitment to the Th17 lineage to promote cell survival and expansion and, potentially, the continued expression of IL-17 and other cytokines that characterize the Th17 phenotype. As presented in Fig. 3, the expression of the *RORγt* gene was significantly weaker in CB-derived $CD4^+$ T cells, whereas the expression of genes encoding IL-23 and the IL-23 receptor did not differ significantly between the $CD4^+$ T cells. Based on the above findings of others, it is possible that the low-level expression of the *RORγt* gene in CB-derived $CD4^+$ T cells is responsible for the absence of *IL-17* mRNA expression in those cells.

Tregs are another functional subset of T cells having anti-inflammatory properties and can cause quiescence of autoimmune diseases and prolongation of transplant function. *In vitro*, Tregs have the ability to inhibit the proliferation and production of cytokines by responder ($CD4^+$ $CD25^-$ and $CD8^+$) T cells subjected to polyclonal stimuli, as well as to down-regulate the responses of $CD8^+$ T cells, NK cells and $CD4^+$ cells to specific antigens.[25,26] These predicates translate *in vivo* to a great number of functions other than the maintenance of tolerance to self-components (prevention of autoimmune disease), such as the ability to prevent transplant rejection. Indeed, donor-specific Tregs can prevent allograft rejection in some models of murine transplant tolerance through a predominant effect on indirect alloresponses.

Foxp3 is thought to be responsible for the development of the Treg population and can act as a phenotypic marker of this fraction.[27] Tregs constitutively express CTLA-4 and there are suggestions that signalling through this pathway may be important for their function, as antibodies to CTLA-4 can inhibit Treg-mediated suppression.[28] As shown above, most of the CB-derived $CD4^+$ T cells were found to express either the *FOXP3* gene or the Foxp3 protein at higher levels compared with PB-derived $CD4^+$ T cells, suggesting that CB-derived $CD4^+$ T cells frequently include a potent Treg population.

As described above, *IL-17* mRNA was more detectable in PB-derived $CD4^+$ cells while *FOXP3* mRNA expression was higher in CB-derived $CD4^+$ cells. Post-transcriptional regulation, as well as differences in mRNA and protein turnover rates, can cause discrepancies between mRNA and protein expression and thus the differences observed in the mRNA expression do not necessary directly indicate those in protein expression.[29] Indeed, we observed some discrepancy between the levels of mRNA and protein with regard to Foxp3 expression in CB-derived $CD4^+$ T cells, as presented above. Nevertheless, changes in mRNA expression are mediated by the alteration of transcriptional regulation, and thus should indicate the differentiation ability of the cells. Therefore, our data indicate that CB-derived $CD4^+$ T cells tend frequently to include potent Tregs, while PB-derived $CD4^+$ T cells tend to include potent IL-17-secreting cells. As described above, DLI with donor CB-derived activated $CD4^+$ T cells is currently becoming established as a routine therapeutic strategy in Japan. It has been proposed that the skewing of responses towards Th17 or Th1 cells and away from Tregs may be responsible for the development and/or progression of autoimmune diseases or acute transplant rejection, and it may thus also be speculated that CB-derived $CD4^+$ T cells are more appropriate for DLI than PB-derived $CD4^+$ T cells.

However, our data also indicate the presence of individual, donor-dependent variations in the characteristics of activated $CD4^+$ T cells derived from CB and PB. More-

over, activated $CD4^+$ T cells do not consist of a single population and should include several distinct functional subsets of $CD4^+$ T cells. Therefore, it is important to clarify the characteristics of activated $CD4^+$ T cells in each preparation to predict the therapeutic effect of DLI in each clinical case.

In summary, our findings demonstrate a difference in gene expression between activated $CD4^+$ T cells derived from CB and those derived from PB. The higher level of *FOXP3* gene expression and the lower level of *IL-17* gene expression in CB-derived $CD4^+$ T cells may indicate that these cells have potential as immunomodulators in DLI therapy. Further detailed analysis should reveal the advantages of activated $CD4^+$ T cells from CB in DLI.

Acknowledgements

We thank the Tokyo Cord Blood Bank for the distribution of cord blood for research use. This work was supported by a grant from the Japan Health Sciences Foundation for Research on Publicly Essential Drugs and Medical Devices (KHC2032), Health and Labour Sciences Research Grants (the 3rd term comprehensive 10-year strategy for cancer control H19-010, Research on Children and Families H18-005, Research on Human Genome Tailor-made and Research on Publicly Essential Drugs and Medical Devices H18-005), and a Grant for Child Health and Development from the Ministry of Health, Labour and Welfare of Japan. It was also supported by CREST, JST.

Disclosures

No competing personal or financial interests exist for any of the authors in relation to this manuscript.

References

1 Loren AW, Porter DL. Donor leukocyte infusions after unrelated donor hematopoietic stem cell transplantation. *Curr Opin Oncol* 2006; **18**:107–14.

2 Roush KS, Hillyer CD. Donor lymphocyte infusion therapy. *Transfus Med Rev* 2002; **16**:161–76.

3 Alyea EP, Soiffer RJ, Canning C *et al.* Toxicity and efficacy of defined doses of CD4(+) donor lymphocytes for treatment of relapse after allogeneic bone marrow transplant. *Blood* 1998; **91**:3671–80.

4 Giralt S, Hester J, Huh Y *et al.* CD8-depleted donor lymphocyte infusion as treatment for relapsed chronic myelogenous leukemia after allogeneic bone marrow transplantation. *Blood* 1995; **86**:4337–43.

5 Tomizawa D, Aoki Y, Nagasawa M *et al.* Novel adopted immunotherapy for mixed chimerism after unrelated cord blood transplantation in Omenn syndrome. *Eur J Haematol* 2005; **75**:441–4.

6 Cohena Y, Nagler A. Hematopoietic stem-cell transplantation using umbilical-cord blood. *Leuk Lymphoma* 2003; **44**:1287–99.

7 Parmar S, Robinson SN, Komanduri K *et al.* Ex vivo expanded umbilical cord blood T cells maintain naive phenotype and TCR diversity. *Cytotherapy* 2006; **8**:149–57.

8 Robinson KL, Ayello J, Hughes R, van de Ven C, Issitt L, Kurtzberg J, Cairo MS. Ex vivo expansion, maturation, and activation of umbilical cord blood-derived T lymphocytes with IL-2, IL-12, anti-CD3, and IL-7. Potential for adoptive cellular immunotherapy post-umbilical cord blood transplantation. *Exp Hematol* 2002; **30**:245–51.

9 Miyagawa Y, Okita H, Nakaijima H *et al.* Inducible expression of chimeric EWS/ETS proteins confers Ewing's family tumor-like phenotypes to human mesenchymal progenitor cells. *Mol Cell Biol* 2008; **28**:2125–37.

10 Werlen G, Hausmann B, Naeher D, Palmer E. Signaling life and death in the thymus: timing is everything. *Science* 2003; **299**:1859–63.

11 Riley JL, June CH. The CD28 family: a T-cell rheostat for therapeutic control of T-cell activation. *Blood* 2005; **105**:13–21.

12 Woo EY, Yeh H, Chu CS, Schlienger K, Carroll RG, Riley JL, Kaiser LR, June CH. Cutting edge: regulatory T cells from lung cancer patients directly inhibit autologous T cell proliferation. *J Immunol* 2002; **168**:4272–6.

13 Azuma H, Yamada Y, Shibuya-Fujiwara N *et al.* Functional evaluation of ex vivo expanded cord blood lymphocytes: possible use for adoptive cellular immunotherapy. *Exp Hematol* 2002; **30**:346–51.

14 Afzali B, Lombardi G, Lechler RI, Lord GM. The role of T helper 17 (Th17) and regulatory T cells (Treg) in human organ transplantation and autoimmune disease. *Clin Exp Immunol* 2007; **148**:32–46.

15 Castellino F, Germain RN. Cooperation between CD4+ and CD8+ T cells: when, where, and how. *Annu Rev Immunol* 2006; **24**:519–40.

16 Reiner SL. Development in motion: helper T cells at work. *Cell* 2007; **129**:33–6.

17 Bi Y, Liu G, Yang R. Th17 cell induction and immune regulatory effects. *J Cell Physiol* 2007; **211**:273–8.

18 Fossiez F, Djossou O, Chomarat P *et al.* T cell interleukin-17 induces stromal cells to produce proinflammatory and hematopoietic cytokines. *J Exp Med* 1996; **183**:2593–603.

19 Loong CC, Hsieh HG, Lui WY, Chen A, Lin CY. Evidence for the early involvement of interleukin 17 in human and experimental renal allograft rejection. *J Pathol* 2002; **197**:322–32.

20 Van Kooten C, Boonstra JG, Paape ME *et al.* Interleukin-17 activates human renal epithelial cells in vitro and is expressed during renal allograft rejection. *J Am Soc Nephrol* 1998; **9**:1526–34.

21 Vanaudenaerde BM, Dupont LJ, Wuyts WA *et al.* The role of interleukin-17 during acute rejection after lung transplantation. *Eur Respir J* 2006; **27**:779–87.

22 Ivanov II, McKenzie BS, Zhou L, Tadokoro CE, Lepelley A, Lafaille JJ, Cua DJ, Littman DR. The orphan nuclear receptor RORgammat directs the differentiation program of proinflammatory IL-17+ T helper cells. *Cell* 2006; **126**:1121–33.

23 Langrish CL, Chen Y, Blumenschein WM *et al.* IL-23 drives a pathogenic T cell population that induces autoimmune inflammation. *J Exp Med* 2005; **201**:233–40.

24 Oppmann B, Lesley R, Blom B *et al.* Novel p19 protein engages IL-12p40 to form a cytokine, IL-23, with biological activities similar as well as distinct from IL-12. *Immunity* 2000; **13**: 715–25.

